ACS APPLIED MATERIALS & INTERFACES

Research Article

www.acsami.org

Synthesis of Au-SiO_2 Asymmetric Clusters and Their Application in ZnO Nanosheet-Based Dye-Sensitized Solar Cells

Hui Li,*[,†] Kaidi Yuan,[‡] Yu Zhang,[†] and John Wang[†]

[†]Department of Materials Science and Engineering, National University of Singapore, Singapore 117576

[‡]National Center of Supervision and Inspection on Solar Photovoltaic Products Quality (CPVT), Wu Xi, China 214028

Supporting Information

ABSTRACT: A facile and novel process modified from the Stöber method has been developed to prepare Au-SiO_2 asymmetric clusters with a number of Au nanoparticles off-center. The Au-SiO_2 asymmetric clusters exhibit the wanted surface plasmons along with increases in the plasmonic near field and optical extinction efficiency. They are incorporated into dye-sensitized solar cells (DSSCs) consisting of ZnO nanosheets as the photoanode, where the surface plasmonic effect on DSSCs performance arising from the Au-SiO_2 asymmetric clusters is investigated. An enhancement in both the photocurrent and overall energy conversion efficiency is observed, arising from the improvement in light harvesting.

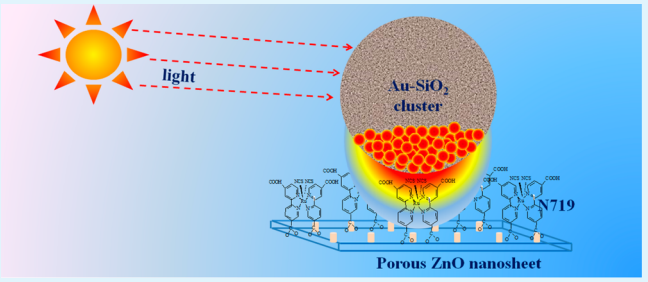

KEYWORDS: *dye-sensitized solar cells, ZnO nanosheets, Au-SiO_2 asymmetric clusters, surface plasmon*

1. INTRODUCTION

Recently, surface plasmon resonance, which is generated when incident light excites coherent oscillation of the free electrons in metal nanoparticles, typically composed of silver or gold, have been shown to be a viable mechanism to enhance the light absorption capability in dye-sensitized solar cells (DSSCs).[1] The metal nanoparticles act as light-harvesting components via excitation of their surface plasmon resonance in the visible range of spectrum. Meanwhile, the coupling of localized surface plasmon resonance (LSPR) with the adsorbed dye will lead to an increase in the effective absorption cross-section of dye molecules. In principle, the LSPR can enhance the light absorption, charge carrier generation, and photocurrent generation, which have been demonstrated with TiO_2 thin films incorporated with silver islands and a sparse coating of gold nanostructure.[2−4] In addition to TiO_2 thin films, LSPR-enhanced photovoltaic performance has also been observed with thick film of TiO_2 nanoparticles incorporated with Ag nanoparticles.[5] It was, however, noted that the photocurrent, photovoltage, and fill factor of DSSCs may be affected by incorporation of bare Au or Ag nanoparticles, when the metal nanoparticles acted as recombination centers or corrosion by the electrolyte took place.[2] To overcome this drawback, Snaith and co-workers[6] applied SiO_2-coated Au core−shell structure into DSSCs consisting of thick films of TiO_2 nanoparticles, and they reported LSPR-enhanced light absorption, photocurrent, and overall energy conversion efficiency. They explained that the SiO_2 layer could avoid the gold nanoparticles as the recombination center, prevent Oswald ripening of Au nanoparticles, and adjust the separation distance between the Au nanoparticle and the chromophore. When the adsorbed dye molecules and the Au nanoparticle are too close, however, energy transfer will happen from the excited dye to the Au nanoparticle.[6] It is well-known that the surface plasmonic near-fields are confined within only a tiny region of the nanometer length scale near the surface of the metal nanoparticles. They decay significantly thereafter, and rule the optical interaction between particles placed in close proximity and the interaction with nearby molecules.[7] If the Au nanoparticle and adsorbed dye molecules is too far then there may be no near-field absorption enhancements in the dye. Therefore, the thickness of SiO_2 coating layer is required to be thin in order to develop a strong optical interaction between Au nanoparticle and the adsorbed dye molecule, and therefore enhance energetic carriers and photocurrent generation in DSSCs. Meanwhile, the hybridization of plasmon modes supported by the individual Au clusters will be generated because of the small separation distance between Au clusters, causing the surface plasmon resonance shift.[8] Thus, to improve the photovoltaic property of DSSCs, SiO_2-coated Au nanostructures should be aimed at both obtaining the strong plasmonic near-field effect on the optical extinction efficiency of dye molecules, and maintaining the surface plasmon modes of individual Au cluster.

In the present study, instead of the conventional Au@SiO_2 core shell structures, we have designed and synthesized a class of asymmetric Au-SiO_2 clusters with a number of Au nanoparticles off-centers. With a number of Au nanoparticles

Received: March 13, 2013
Accepted: May 22, 2013
Published: May 22, 2013

   dx.doi.org/10.1021/am400914g | ACS Appl. Mater. Interfaces 2013, 5, 5601−5608

assembled in the asymmetric Au-SiO_2 clusters, the intensity of plasmonic near field and extinction efficiency of Au nanoparticles at Au nanoparticle grain boundary will be increased because of the coupling of the surface plasmon near-field of each Au nanoparticle.[9] Meanwhile, the asymmetric Au-SiO_2 clusters include both the thinner SiO_2 layer side, where a strong optical interaction between Au nanoparticles and adsorbed dye molecules can be developed, and the thicker SiO_2 layer side, where the surface plasmon mode of individual Au cluster can be maintained. To the best of our knowledge, few studies have been made of the synthesis of Au-SiO_2 asymmetric clusters with a number of Au nanoparticles off-centers and investigation into the effect of surface plasmons on the enhancement of photocurrent and energy conversion efficiency in DSSCs based on porous ZnO nanosheets. Porous ZnO 2D nanosheets have received extensive interests, in attempts to improve the overall photovoltaic performance of DSSCs on account of the fact that they have a relatively high specific surface area together with an effective electron and electrolyte diffusion, resulting in a decrease in both the series resistance and the recombination rate of the cell.[10] However, the energy conversion efficiency of DSSCs based on porous ZnO 2D nanosheets is largely underdeveloped because of the difficulty in achieving a dense structure, which is required for the light-harvesting capability. The LSPR enhancement on the light absorption of DSSCs is more significant with the loose ZnO nanosheets as compared to that of the dense film structure. Light can be well-reflected in the porous ZnO nanosheets, after the incorporation of metal nanoparticles. The shadowing of metal nanoparticles in a dense structure cannot be avoided, leading to restricted light penetration into the film. Here, we first describe a facile and novel process modified from the Stöber method to prepare Au-SiO_2 asymmetric clusters with Au nanoparticles being positioned off-center. Then, we will incorporate these as-prepared Au-SiO_2 asymmetric clusters into ZnO nanosheet photoanode. Finally, we will further demonstrate the effect of these Au-SiO_2 asymmetric clusters on the photocurrent and energy conversion efficiency in DSSCs device of ZnO nanosheet structures.

2. EXPERIMENTAL PROCEDURE

Materials. Hydrogen tetrachloroaurate ($HAuCl_4 \cdot 3H_2O$, Sigma-Aldrich, St. Louis, MO), toluene (Riedel-deHaen), tetraoctylammonium bromide (TOAB, Aldrich, St. Louis, MO), sodium borohydride ($NaBH_4$, Merck, Whitehouse Station, NJ), dodecanethiol (DDT, Aldrich, St. Louis, MO), block copolymer Pluronic F127 ($EO_{106}PO_{70}EO_{106}$, Sigma, St. Louis, MO), tetramethoxysilane (TMOS, 98%, Aldrich, St. Louis, MO), tetrahydrofuran (THF, Fisher Science, Singapore), Zinc acetate hydrate ($Zn(CH_3COO)_2 \cdot 2H_2O$, 98%, Alfar Aesar, Ward Hill, MA), Ethylenediamine (EDA; Merck, Whitehouse Station, NJ) were purchased. All the chemicals were not further purified before use.

Synthesis of Au-SiO_2 Asymmetric Clusters. In a typical synthesis,[11] 90 mg of F127 was dissolved in 800 μL of THF and mixed with 100 μL of the dodecanethiol surface-coated Au stock solution, synthesized in a two-phase liquid–liquid system.[12] The mixtures were stirred at room temperature for 12 h before adding TMOS (23 μL). Subsequently, the mixture was vortexed and sonicated for 1 min, and then injected slowly into 10 g of deionized water (DI water) while being stirred at 700 rpm. The stirring was continued for an additional 4 days to evaporate THF and ensure a complete hydrolysis of TMOS. The resultant aqueous dispersion of Au-SiO_2 asymmetric clusters was then dialyzed for 24 h against DI water using an MWCO 8000 dialysis tube to remove the unreacted silica precursors.

Preparation of ZnO Nanosheets. ZnO nanosheets were prepared by a wet-chemical method, the typical procedure of which is described as follows:[13] 20 mL of 0.125 M $Zn(CH_3COO)_2 \cdot 2H_2O$ solution was first prepared and stirred at room temperature for 10 min to obtain a clear solution. 0.5 grams of surfactant F127 was then added into the zinc acetate solution, stirred at room temperature for about 1 h to dissolve the surfactant F127, and obtain a clear solution; 0.125 M EDA solution was then added into the above clear zinc acetate solution with F127. The solution became turbid immediately after adding EDA solution. The turbid solution was kept at room temperature for 2 h with stirring, and then aged at room temperature for 12 h. The resultant white precipitates were centrifuged with 8000 rpm for 6 min. After centrifugation, the precipitates were put into an oven for thermal treatment at 300 °C for 1 h at a heating rate 1 °C/min.

ZnO Photoanode and ZnO with Au-SiO_2 Asymmetric Cluster Incorporated. An appropriate amount of ZnO powder consisting of nanosheets was dispersed in organic binders with weight ratio 11%,[14] incorporating a specified amount of Au-SiO_2 asymmetric clusters. ZnO films were prepared by a doctor blading method,[15] which was described in the ref 14.

Characterizations. The morphologies of the Au-SiO_2 clusters were investigated by transmission electron microscopy (TEM, JEOL JEM-2010F, JEOL, Tokyo, Japan), and the chemical structures of the as-prepared Au nanoparticles, Au-SiO_2 clusters and ZnO with or without Au-SiO_2 clusters were studied using Fourier transform infrared spectroscopy (FT-IR, Varian 3100 Excalibur, Palo Alto, CA). The optical behavior of Au nanoparticles, Au-SiO_2 asymmetric clusters and the amount of dye loading were measured by using UV–vis-NIR spectrophotometer (Cary 5000, Varian, Santa Clara, CA). Photovoltaic performance of the DSSCs thus assembled was characterized on an active area of 0.35 cm^2 by using a Keithley 2420 sourcemeter under AM1.5 100 mW/cm^2 illumination. The irradiance source was a 150 W NREL traceable Oriel Class AAA solar simulator (model 92250A-1000). Incident photon-to-current conversion efficiency (IPCE) was measured by a DC method. The light source was a 300 W xenon Lamp (Oriel 6258) coupled with a flux controller to improve the irradiance stability. The light beam passed through a monochromator (Cornerstone 260 Oriel 74125) to select a single wavelength with a resolution of 10 nm. Light intensity was measured by a NREL traceable Si detector (Oriel 71030NS, Newport, Irvine, CA), while the short circuit currents of the DSSCs were measured by an optical power meter (Oriel 70310).

Simulation of Extinction Spectra, Plasmonic Near-Field Maps. Simulations of the optical extinction spectra were performed using the discrete dipole approximation (DDA) implemented in DDSCAT 7.22 software.[16] The dipoles were distributed within spheres that represent the shapes of the asymmetrical Au-SiO_2 clusters. The characteristic dimensions of the gold nanoparticles and SiO_2 spheres were determined from large-ensemble TEM measurement. Plasmonic near-field maps were simulated at the LSPR wavelengths using the ddfield routine of the DDSCAT 7.22 package. All maps were generated outside the gold nanoparticles at the minimum distance of 1 nm from the gold surface and with incident polarization along the x-axis.

3. RESULTS AND DISCUSSION

Asymmetric clusters have attracted considerable interests owing to their potential in several applications, such as in optical, optoelectronic, and sensing devices.[17] Although certain progress has been made in developing the asymmetric, hybrid colloidal clusters, so far few studies have been reported for Au-SiO_2 asymmetric clusters with a number of Au nanoparticles positioned off-center. In the present work, we have developed a process modified from the Stöber method to synthesize the Au-SiO_2 asymmetric clusters. A common route for synthesis of asymmetric structure is to utilize an active surface, such as a liquid–liquid or liquid–solid interface, to expose the two sides

of a particle to different chemical environments.[18] Here, the essential idea behind our approach is to form the Au-SiO_2 asymmetric clusters at the interface. Figure 1 shows the scheme

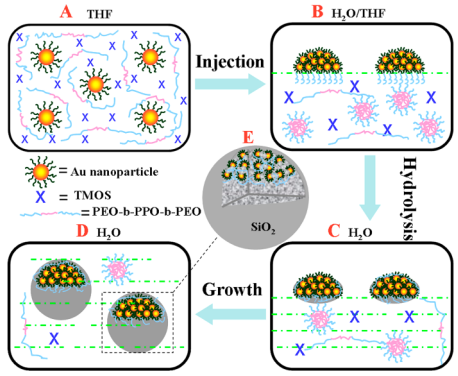

Figure 1. Scheme showing the formation of Au-SiO_2 asymmetric clusters by a process modified from the Stöber method.

of interfacial formation of the Au-SiO_2 asymmetric clusters. To start with, F127, a commercially available representative of nonionic PEO-based block copolymers, preprepared hydrophobic dodecanethiol-coated Au nanoparticles of ~3 nm in diameter, and silica precursor TMOS are mixed and well-dispersed in THF (Figure 1A). Upon injecting the mixture solution into an aqueous environment, the hydrophobic Au nanoparticles tend to aggregate together prior to the coating process, and form a hemisphere with curvature, in order to lower the hydrophobic–hydrophilic interfacial energy. Meanwhile, the morphology of the aggregated Au nanoparticles is independent of the amounts of surfactant F127 and Au nanoparticles added (shown in Figures S1 and S2 in the Supporting Information, respectively), when the curvature is largely decided by the intrinsic behavior of dodecanethiol and water. The same phenomena have been observed by Sastry and co-workers.[19] It is known that the hydrophobic hemisphere Au nanostructures are not stable in the aqueous environment without surface modification. At the same time, the Au nanoparticles exhibit a weak affinity toward silica, the deposition and adhesion of silica on the Au nanoparticles surface is relatively hard in the absence of primer.[20] Here, we employ surfactant F127 as the stabilizer and primer, where the PPO chains of F127 will interact with the hydrophobic dodecanethiol chains on the surface of Au nanoparticles, and the PEO chains of F127 will be exposed to water to minimize the interfacial energy between the aggregated hydrophobic Au nanoparticles and water. Polymeric micelles of F127 will form and TMOS is dispersed in the water solution with the protection of F127 (Figure 1B). Consequently, the hydrolysis reaction of TMOS takes place, and the resultant silica phase is apt to attach on the surface of hemisphere Au aggregation with F127 via hydrogen bonding.[21] The hydrogen bonding is formed between the silanol group of hydrolyzed TMOS and the PEO chains of F127 surfactant. Subsequently, the silanol groups condense on the surface of aggregated Au hemispheres to form a thin silica layer (Figure 1C). To demonstrate the role of surfactant F127, we prepared a sample without F127 by keeping the other parameters unchanged, and observed that only aggregated Au nanostructure is formed without silica shell (see Figure S3 in the Supporting Information). The fact that the surfactant F127 affected the silica deposition strongly supports the growth theory via hydrogen bonding. As the process proceeds, the unreacted TMOS in the solution will undergo further hydrolysis and condensation on the outer surface of the silica shell, forming the Au-SiO_2 asymmetrical clusters with aggregated Au nanoparticles being positioned off-center (Figure 1D). The resultant Au-SiO_2 asymmetric clusters consist of two parts, namely the silica sphere and Au aggregation (Figure 1E) embedded in the silica. This facile and novel process modified from the Stöber method has several advantages, including for example: (i) simple, the hydrophobic Au nanoparticles are directly coated by silica without ligand exchange; (ii) benign, the Au-SiO_2 asymmetric clusters can be successfully formed in an aqueous solution at room temperature. As discussed below, the Au-SiO_2 asymmetric clusters can be applied in the DSSCs, where the overall performance is improved and the important features of Au-SiO_2 asymmetric clusters are described.

To prove the above proposed growth mechanism for the asymmetry Au-SiO_2 clusters, the steps involved in the synthesis process were monitored at different stages. TEM images of the samples synthesized at reaction time of 8 h, 24 h, 2 d, and 4 d are shown in Figure 2a–d, respectively. It can be seen that the

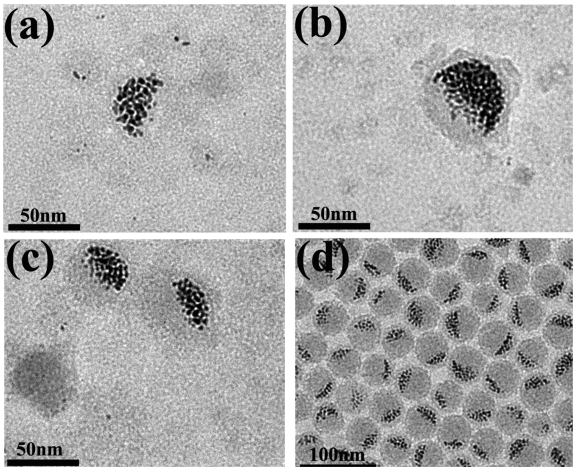

Figure 2. TEM images showing the as-synthesized Au-SiO_2 asymmetric clusters at different stages of reaction time: (a) 8, (b) 24, (c) 48, and (d) 96 h.

aggregated Au hemispheres were initially formed because of the intrinsic behavior of dodecanethiol and water (Figure 2a). A thin layer of silica then grew on the surface of Au hemispheres in the presence of surfactant F127 (Figure 2b), and the silica deposition on the silica layer occurs with the further hydrolysis of TMOS (Figure 2c), followed by the development of a spherical morphology at the late stage (Figure 2d).

Figure 3a further characterizes the morphology of the as-synthesized asymmetric Au-SiO_2 clusters. It can be seen that there is a clear contrast between the gray silica and dark Au nanoparticles. The clusters are rather uniform in dimensions, i.e., about 40 nm with rather identical structure, where each contains a number of aggregated Au nanoparticles on one side of the cluster. It also can be seen that the cluster size is largely determined by the curvature of the Au hemisphere, and the curvature of Au hemisphere is decided by the intrinsic behavior of dodecanethiol and water, which can explain the formation of uniform clusters obtained on a large scale. A high magnification TEM image of typical Au-SiO_2 asymmetric clusters is shown in Figure 3b, where one can see that the aggregated Au

dx.doi.org/10.1021/am400914g | ACS Appl. Mater. Interfaces 2013, 5, 5601–5608

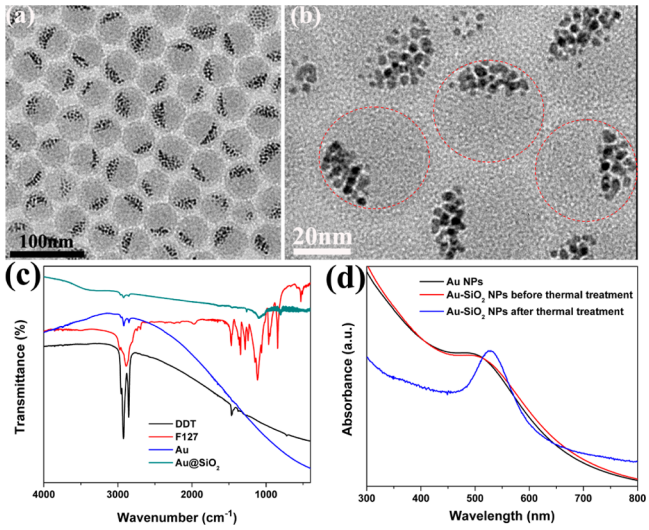

Figure 3. (a) TEM image showing the as-synthesized Au@SiO_2 asymmetric clusters; (b) a high-magnification image of the as-synthesized Au@SiO_2 asymmetric clusters; (c) FT-IR spectra of DDT, F127, Au nanoparticles, and Au@SiO_2 asymmetric clusters; (d) UV−vis spectra of Au nanoparticles and Au@SiO_2 asymmetric clusters before and after thermal treatment.

nanoparticles are individually dispersed and do not show multiply twinned morphology, due to the protection from the dodecanethiol groups on their surfaces.[12] The silica shell is initially grown on the surface of aggregated Au nanoparticle hemispheres, as illustrated in Figure 1. The chemical structure of Au-SiO_2 asymmetric clusters were further characterized using FT-IR spectroscopy, as shown in Figure 3c over the wavelength range of 4000−400 cm^{-1}. It can be seen that the peaks at 2850 and 2920 cm^{-1} are contributions from the C−H of CH_2 group symmetric and the antisymmetric vibrations of DDT and F127 molecules. The small peak at 1262 cm^{-1} corresponds to the C−H stretching of surfactant F127. The peak at 1100 cm^{-1} arises from the Si−O−Si antisymmetric stretching.[22] The presence of the characteristic bands of silica, F127 block copolymers and DDT, confirms the hybrid structure of the silica-Au asymmetric clusters, as shown in Figure 1E. The morphologies of the Au-SiO_2 clusters before and after annealing are shown in Figure S4 in the Supporting Information. We have characterized the optical behavior of the as-synthesized Au nanoparticles, and Au-SiO_2 asymmetric clusters before and after annealing using UV−vis spectroscopy. As shown in Figure 3d, there is an obvious visible-light absorbance at ∼500 nm for both the as-synthesized Au nanoparticles and the Au-SiO_2 asymmetry clusters, indicating the occurrence of LSPR with both samples. The LSPR peak does not shift for the as-synthesized Au nanoparticles and Au-SiO_2 asymmetric clusters, which suggests that the aggregated Au nanoparticles are individually dispersed in the Au-SiO_2 asymmetric clusters, in a good agreement with the TEM observations (shown in Figure S4a in the Supporting Information). Upon thermal annealing at 400 °C for 20 min, the visible-light absorption is red-shifted to ∼530 nm because of the decomposition of the DDT group, where the overall refractive index of the surface layer has changed.[23,24] The secondary growth of Au nanoparticles is shown in Figure S4b in the Supporting Information.

Previous experimental and theoretical work mainly focused on the LSPR of core shelled Au-SiO_2 or Janus structure with single Au nanoparticle. Little work has been reported for the LSPR of asymmetric Au-SiO_2 clusters with a number of Au nanoparticles off-center. To illustrate the distinct optical behavior of the asymmetric Au-SiO_2 clusters with a number of Au nanoparticles off-center, we simulated the plasmonic near-field maps for the Au-SiO_2 asymmetric clusters with one, three, and seven Au nanoparticles off-center at the LSPR wavelengths using the ddfield routine of the DDSCAT 7.22 software, and the optical extinction spectra were simulated using DDA, as shown in Figure 4, along with a simple

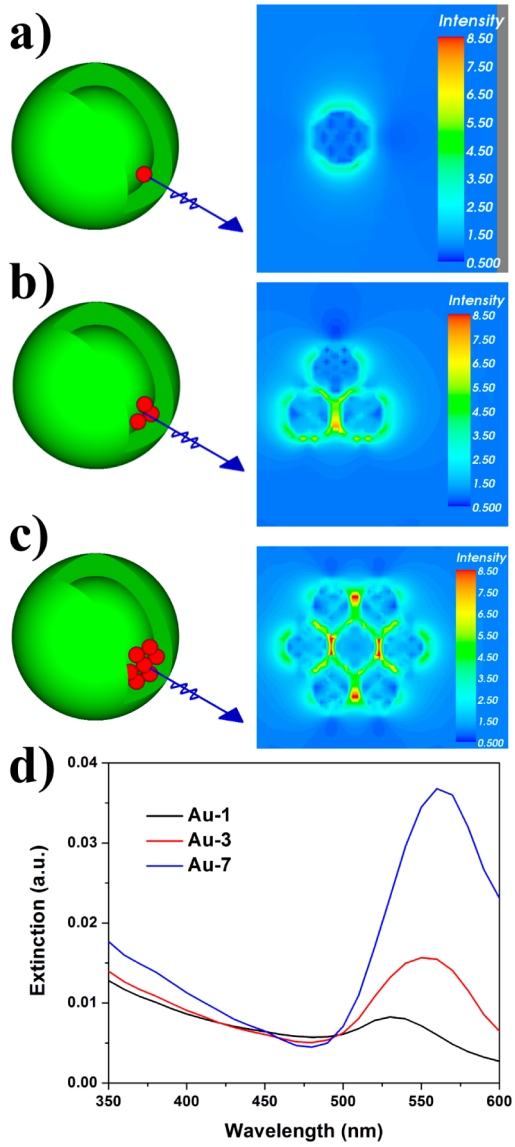

Figure 4. Plasmonic near-field maps (cross-section view at $x = 0$, incident light from x direction and polarization along y axis) simulated using DDA for the Au-SiO_2 asymmetric clusters with different amounts of Au nanoparticles: (a) one Au nanoparticle; (b) three Au nanoparticles; and (c) seven Au nanoparticles, (d) optical extinction spectra.

morphology scheme. The green sphere represents SiO_2, and the red small spheres represent Au nanoparticles, which are well-dispersed in the SiO_2 sphere. A weak plasmon near-field intensity was obtained from the plasmonic near-field map of the asymmetry Au-SiO_2 clusters with one Au nanoparticle off-center, and a surface plasmon resonance at 530 nm was observed from the optical extinction spectrum. Compared to

dx.doi.org/10.1021/am400914g | ACS Appl. Mater. Interfaces 2013, 5, 5601−5608

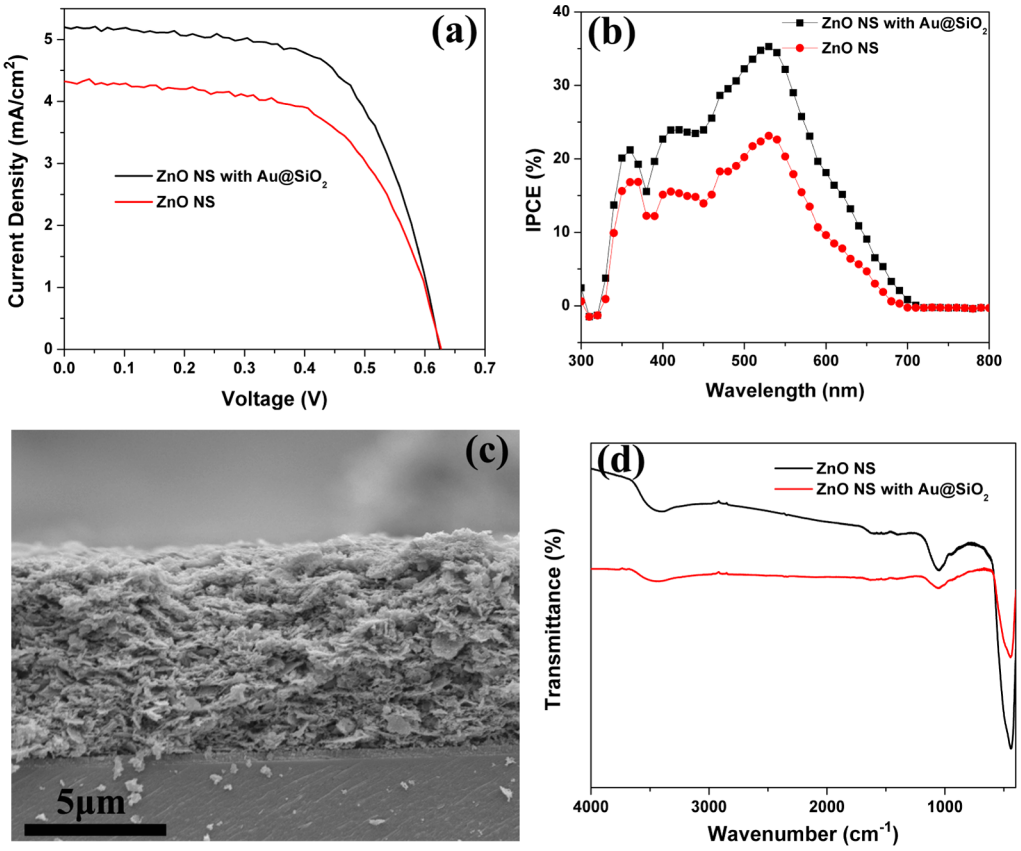

Figure 5. (a) $J-V$ curves and (b) IPCE spectra of the DSSC devices made of ZnO nanosheets with and without Au-SiO_2 asymmetric clusters. (c) Cross-sectional SEM image of the DSSC device made of ZnO nanosheets without Au-SiO_2 asymmetric clusters. (d) FT-IR spectra of ZnO nanosheets with and without Au-SiO_2 asymmetric clusters.

the clusters with one Au nanoparticle, the asymmetry Au-SiO_2 clusters with three or seven Au nanoparticles displayed greatly enhanced plasmonic near-field intensity at the boundary between Au nanoparticles, as shown in Figure 4b, c, which can be explained by the plasmonic near-field coupling in Au dimers.[9] At the same time, the optical extinction efficiency was enhanced with increasing the number of Au nanoparticles, as shown in Figure 4d, in a good agreement with the plasmonic near-field maps, shown in Figure 4a–c. In addition, the LSPR peaks shifted from 530 nm to around 560 nm with the increasing number of Au nanoparticles because of the near field coupling between Au nanoparticles. The observed difference between the simulated optical extinction spectra using DDA at 560 nm and the experimental results at 530 nm can be accounted for by the number (3–7) of Au nanoparticles. The parameters that control the as-prepared asymmetry Au-SiO_2 clusters with a number of Au nanoparticles off-center are rather complicated. Indeed, it has been reported for the enhanced optical extinction efficiency of Au dimers deposited on a substrate using electron beam lithography.[9] For the asymmetry Au-SiO_2 clusters with an appropriate amount of Au nanoparticles, the local optical fields in the interstitial space between two Au nanoparticles can be strongly enhanced by 4–5 times, as compared to the plasmonic near field intensity for asymmetry Au-SiO_2 clusters with a single Au nanoparticle. It would therefore be of interest to investigate the Au-SiO_2 clusters with a number of Au nanoparticles off-center for visible-light harvesting.

An enhanced light harvesting and stronger interaction between Au nanoparticle and chromophore would be able to enhance the overall energy conversion efficiency in DSSCs. In several recent studies, considerable efforts have been made to apply the Au-SiO_2 nano core–shell structures to DSSCs to enhance the light harvesting and the overall photovoltaic performance. Different from those studies using Au-SiO_2 nano core shells, we incorporated Au-SiO_2 asymmetric clusters into DSSCs by using ZnO nanosheets as the photoanode. Figure 5a shows the current voltage ($J-V$) curves for DSSCs by employing N719 ruthenium sensitizer with 8.3 μm thick ZnO nanosheet/Au-SiO_2 asymmetric clusters. The photovoltaic parameters measured for the DSSC cells were summarized in Table 1. The fill factor and the open-circuit voltage did not change much by incorporating the Au-SiO_2 asymmetric clusters into ZnO nanosheets. It suggests that the presence of the Au-SiO_2 asymmetric clusters does not create more recombination centers. However, the overall conversion efficiency of DSSCs was improved when the Au-SiO_2 asymmetric clusters were added, where the photocurrent was apparently enhanced, indicating that the surface plasmons arising from the Au-SiO_2

Table 1. Photovoltaic Parameters of the DSSCs Devices Made of ZnO Nanosheets with and without Au-SiO_2 Asymmetric Clusters

samples	V_{oc} (V)	J_{sc} (mA/cm^2)	ff (%)	η (%)	dye amount (mol/cm^2)
ZnO NS with Au-SiO_2	0.62	5.82	62.1	2.24	1.66×10^{-07}
ZnO NS	0.62	4.81	60	1.79	1.68×10^{-07}

dx.doi.org/10.1021/am400914g | ACS Appl. Mater. Interfaces 2013, 5, 5601–5608

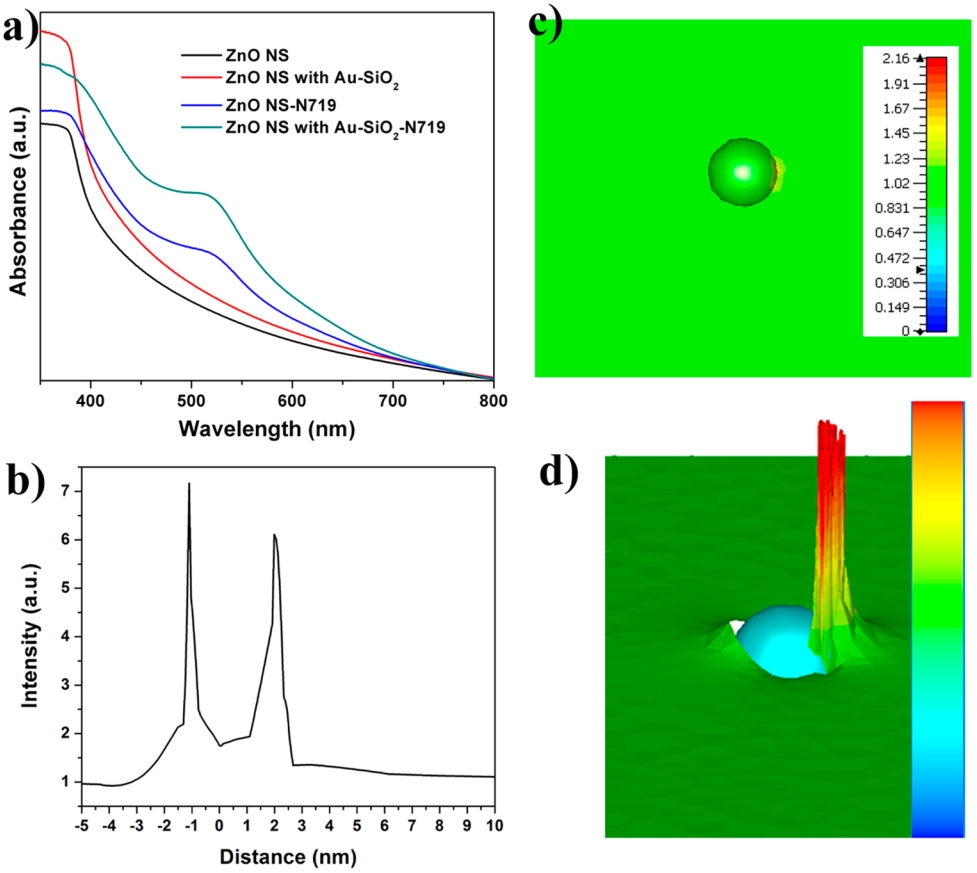

Figure 6. (a) UV−vis absorption spectra of the ZnO nanosheet film with or without Au-SiO_2 clusters before and after dye loading; (b) enhancement in the electric field intensity at the LSPR peak wavelength as a function of distance; (c) plasmonic near-field map; (d) plasmonic near-field isoplanar map.

clusters have contributed to the overall light harvesting and the photocurrent generation. The incident photon-to-current conversion (IPCE) spectra show that the DSSC device incorporated with Au-SiO_2 clusters possessed much higher internal quantum efficiency than the one without Au-SiO_2 incorporation, as shown in Figure 5b. It can be seen that the photocurrent peaks mainly occur in the visible-light range at approximately 530 nm contributed by the dye absorption with values of 22, and 35% for ZnO film and ZnO film with Au-SiO_2 clusters, respectively. That is, the IPCE obtained for the ZnO film with Au-SiO_2 cluster is almost 1.6 times of that of the ZnO film. IPCE can be expressed in terms of the light-harvesting efficiency (LHE), the quantum yield of charge injection from the excited dye to the semiconductor, and the collection efficiency of injected electrons at the back contact. As discussed above, the ZnO films with or without Au-SiO_2 clusters have similar nanostructures and electronic behavior. Since the same dye and electrolyte were employed in the DSSC fabrication, the internal quantum efficiency is expected to be similar for the ZnO films with or without Au-SiO_2 clusters. The difference in IPCE shall be largely related to the light harvesting efficiency, which confirms the surface plasmonic enhanced photocurrent and overall energy conversion efficiency, as shown by the $J-V$ curves. Up to now, the plasmonic enhanced photovoltaic properties were only observed for DSSCs with film thicknesses less than 1 μm.[2−6] The shadowing effect cannot be avoided in thick dense films, leading to restricted light penetration into the films. In the present study, the DSSC device with a ZnO nanosheets electrode of ∼8.3 μm in thickness possesses a loose structure, as shown in Figure 5c. It demonstrates a plasmonic enhanced photocurrent by ensuring a good light reflection in such thick yet porous films after being incorporated with Au-SiO_2 asymmetric clusters. It also indicates that photons absorbed by the asymmetry Au-SiO_2 clusters have been successfully converted to electrons in DSSCs.[25] In addition, the chemical structures of both the ZnO nanosheets and the ZnO nanosheets with Au-SiO_2 asymmetric clusters were measured by FT-IR spectra, as shown in Figure 5d. Both show similar FT-IR spectra, indicating that there is no additional bond formed in the ZnO nanosheet structure after incorporation of Au-SiO_2 clusters. There is a strong plasmonic near-field for the asymmetry Au-SiO_2 clusters with a number of Au nanopariticles, as shown in Figure 4. Therefore, when compared to the conventional Au-SiO_2 core−shells or Janus structure with one single Au nanoparticle, the asymmetric Au-SiO_2 clusters will greatly enhance the interaction between Au nanoparticles and adsorbed dye molecules via the strong surface plasmonic near-field, leading to an increase in the extinction efficiency of dye molecules. It has been reported that the LSPR wavelength peak of Au dimer shifts due to the near-field coupling between Au nanoparticles, and that the shift decays almost exponentially with increasing Au nanoparticle spacing and become negligible when the gap between the Au nanoparticles exceeds about 2.5 times of the particle short-axis length.[26] For the Au-SiO_2 asymmetric clusters, the SiO_2 spheres have diameters of about 40 nm, which is much larger than those of the aggregated Au clusters. Therefore, the LSPR shift can be ignored and the plasmon mode at 530 nm supported by the

dx.doi.org/10.1021/am400914g | ACS Appl. Mater. Interfaces 2013, 5, 5601−5608

individual asymmetry Au-SiO_2 clusters can be maintained when two asymmetric Au-SiO_2 clusters touch with each other in the ZnO film. At the same time, this plasmon mode of individual asymmetric Au-SiO_2 clusters with a number of Au nanoparticles at 530 nm matches the dye N719 absorption position very well.

To prove the effect of LSPR on the enhancement of light harvesting capability, the optical absorption spectra of the ZnO nanosheet film and the ZnO nanosheet film with Au-SiO_2 clusters before and after dye loading were shown in Figure 6a. They clearly show the effectively enhanced incident light absorption in the ZnO nanosheet film with Au-SiO_2 clusters, when compared to that of the ZnO nanosheet film before and after dye loading, respectively. In principle, metal nanoparticles could enhance the light absorption by either scattering light enabling a longer optical path-length, the direct dipole−dipole interaction, or the near-field coupling between the surface plasmon polariton and the dye excited state. It is well-known that the light scattering of metal nanoparticles is related to their particle sizes, i.e., a larger metal particle size gives rise to a stronger light scattering effect.[27] Snaith et al.[6] have reported a negligible effect of light scattering of Au-SiO_2 nanostructures on the enhancements of light absorption. Moreover, in the present study, the amount of Au-SiO_2 clusters in the DSSC device is small, suggesting that the enhancement of light harvesting is not due to the light scattering. The two remaining possibilities are the discrete energy transfer from the plasmon mode to the dye excited state, or the direct near field coupling between the surface plasmonic resonance and the dye excited state. The former is unlikely due to the existence of an insulator layer of SiO_2.[28] Thus, the light-harvesting efficiency in the ZnO nanosheet films with Au-SiO_2 clusters was improved mainly by the direct interaction between surface plasmonic near-field and adsorbed dye molecules. The plasmonic near-field maps of asymmetric Au-SiO_2 cluster with a number of Au nanoparticles were shown in Figure 6c, d. It is known that the Au nanoparticles can be used as an effective 'antenna' for the incident sunlight that stores the incident energy in a localized surface plasmon mode. Indeed, a strong LSPR around the Au clusters is observed in Figure 6c, d, which led to an intensified plasmonic near-field and hence a higher optical absorption in ZnO photoanode. To prove the near-field effect on the increase in extinction cross-section of adsorbed dye molecules, leading to the enhanced light harvesting, the plasmonic near-field distribution is taken into consideration and is shown in Figure 6b. There is a fast decay of the near-field, and the near-field effect disappears within 2 nm from the Au nanoparticle surface. In the asymmetric Au-SiO_2 clusters, the thickness of the SiO_2 layer on the Au cluster side is about 1 nm, which means that the effective interaction between the LSPR from Au nanoparticles and the adsorbed dye molecules occurs. The increase in the photocurrent density and the overall energy conversion efficiency for the ZnO nanosheet films with Au-SiO_2 clusters can thus be explained on the basis of the enhanced light-harvesting capability, because of the near-field coupling between the surface plasmon polariton and the dye excited state.

To further confirm that the enhanced light harvesting efficiency is derived from the surface plasmonic effect of Au-SiO_2 nanoclusters, the amount of adsorbed dye in both devices (bare ZnO nanosheet film and ZnO nanosheet film with asymmetric Au-SiO_2 clusters) was investigated, as summarized in Table 1. The dye can be desorbed into 1.0 mM NaOH solution by keeping the dye-adsorbed films in NaOH solution for 1 h to make sure most of the dye is desorbed. The absorption spectra of the desorbed dye are shown in Figure 7,

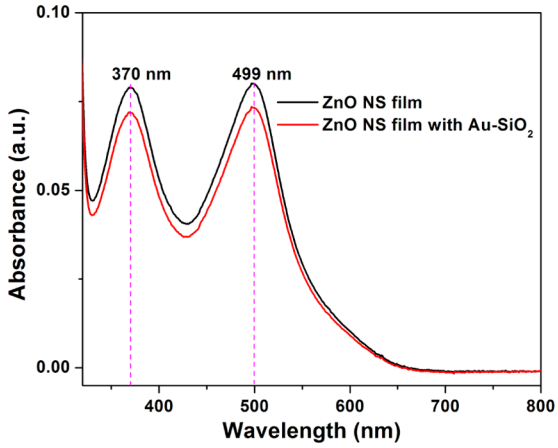

Figure 7. UV−vis absorption spectra of the dye desorbed from the bare ZnO nanosheet film and the ZnO nanosheet film with Au-SiO_2 clusters.

where the peaks located at 370 and 499 nm can be observed, which correspond to N719 dye in 1.0 mM NaOH solution. There is a larger absorbance value for the bare ZnO nanosheet films than that for the ZnO nanosheet films with asymmetric Au-SiO_2 cluster, which means that the presence of Au-SiO_2 clusters has decreased the dye adsorption on the surface of ZnO nanosheets. Therefore, the increased current density and energy conversion efficiency is not an effect of the dye adsorption. It is the LSPR enhanced light-harvesting capability in DSSCs.

4. CONCLUSION

We have successfully developed a class of Au-SiO_2 asymmetric clusters with a number of Au nanoparticles positioned off-center via a facile route modified from the Stöber method in aqueous solution. The Au-SiO_2 asymmetric clusters exhibit a strong optical extinction efficiency and plamonic near-field effect due to the localized surface plasmon resonance coupling between the Au nanoparticles in the Au-SiO_2 asymmetric clusters. The strong optical interaction between Au clusters and adsorbed dye molecules thus obtained can enhance the light harvesting capability from the thinner SiO_2 side, and the surface plamson resonance shift can be avoided from the thicker SiO_2 side when two Au-SiO_2 clusters touch with each other. A plasmonic effect in photocurrent and overall energy conversion efficiency has been demonstrated for DSSCs by incorporating these Au-SiO_2 asymmetric clusters into the thick ZnO nanosheet film. As a result of the improved light harvesting efficiency by the surface plasmonic effect of Au-SiO_2 asymmetric clusters, an enhancement in both photocurrent density and energy conversion efficiency was observed.

■ ASSOCIATED CONTENT

Supporting Information

TEM images of the Au-SiO_2 asymmetric clusters derived from different amounts of F127, Au-SiO_2 asymmetric clusters with different amounts of Au nanoparticles, a Au-SiO_2 cluster prepared in the absence of surfactant F127, and Au-SiO_2 clusters before and after thermal treatment. This material is available free of charge via the Internet at http://pubs.acs.org/

AUTHOR INFORMATION

Corresponding Author

*hone: +65 65167778. Fax: +65 67763604. E-mail: g0800325@nus.edu.sg.

Notes

The authors declare no competing financial interest.

ACKNOWLEDGMENTS

The authors thank Mr. Karvianto for his suggestion in the plasmonic near-field simulation work. This work is supported by the Agency for Science, Technology and Research (A*Star, Singapore, Grant numbers: 072 101 0013 and 1121202013), and MOE (T11-0702-P06), conducted at the National University of Singapore.

REFERENCES

(1) Atwater, H. A.; Polman, A. *Nat. Mater.* **2010**, *9*, 205−213.
(2) Standridge, S. D.; Schatz, G. C.; Hupp, J. T. *J. Am. Chem. Soc.* **2009**, *131*, 8407−8409.
(3) Zhao, G.; Kozuka, H.; Yoko, T. *Sol. Energy Mater. Sol. Cells* **1997**, *46*, 219−231.
(4) Hägglund, C.; Zäch, M.; Kasemo, B. *Appl. Phys. Lett.* **2008**, *92*, 013113 (1−3)..
(5) Lin, S. J.; Lee, K. C.; Wu, J. L.; Wu, J. Y. *Appl. Phys. Lett.* **2011**, *99*, 043306 (1−3)..
(6) Brown, M. D.; Suteewong, T.; Kumar, R. S. S.; D'Innocenzo, V.; Petrozza, A.; Lee, M. M.; Wiesner, U.; Snaith, H. J. *Nano Lett.* **2011**, *11*, 438−445.
(7) Myroshnychenko, V.; Rodríguez-Fernández, J.; Pastoriza-Santos, I.; Funston, A. M.; Novo, C.; Mulvaney, P.; Liz-Marzán, L. M.; García de Abajo, F. J. *Chem. Soc. Rev.* **2008**, *37*, 1792−1805.
(8) Yang, S. C.; Kobori, H.; He, C. L.; Lin, M. H.; Chen, H. Y.; Li, C. C.; Kanehara, M.; Teranishi, T.; Gwo, S. *Nano Lett.* **2010**, *10*, 632−637.
(9) Jain, P. K.; Huang, W. Y.; EI-Sayer, M. A. *Nano Lett.* **2007**, *7*, 2080−2088.
(10) Hosono, E.; Fujihara, S.; Honma, T.; Zhou, H. S. *Adv. Mater.* **2005**, *17*, 2091−2094.
(11) Tan, H.; Liu, N. S.; He, B. P.; Wong, S. Y.; Chen, Z. K.; Li, X.; Wang, J. *Chem. Commun.* **2009**, *41*, 6240−6242.
(12) Brust, M.; Walker, M.; Bethell, D.; Schiffrin, D. J.; Whyman, R. *J. Chem. Soc., Chem. Commun.* **1994**, *7*, 801−802.
(13) Li, H.; Zhang, Y.; Wang, J. *J. Am. Ceram. Soc.* **2012**, *95*, 1241−1246.
(14) Li, H.; Xie, Z. B.; Zhang, Y.; Wang, J. *Thin Solid Films* **2010**, *518*, e68−e71.
(15) Keis, K.; Magnusson, E.; Lindström, H.; Lindquist, S. E.; Hagfeldt, A. *Sol. Energy Mater. Sol. Cells* **2002**, *73*, 51−58.
(16) Draine, B. T.; Flatau, P. J. *J. Opt. Soc. Am. A* **1994**, *11*, 1491−1499.
(17) Ohnuma, A.; Cho, E. C.; Camargo, P. H. C.; Au, L.; Ohtani, B.; Xia, Y. N. *J. Am. Chem. Soc.* **2009**, *131*, 1352−1353.
(18) Paunov, V. N.; Cayre, L. J. *Adv. Mater.* **2004**, *16*, 788−791.
(19) Swami, A.; Kasture, M.; Pasricha, R.; Sastry, M. *J. Mater. Chem.* **2004**, *14*, 709−714.
(20) Han, Y.; Jiang, J.; Lee, S. S.; Ying, J. Y. *Langmuir* **2008**, *24*, 5842−5848.
(21) Zhao, D. Y.; Feng, J. L.; Huo, Q. S.; Melosh, N.; Fredrickson, G. H.; Chmelka, B. F.; Stucky, G. D. *Science* **1998**, *279*, 548−552.
(22) Ma, D.; Li, M.; Patil, A. J.; Mann, S. *Adv. Mater.* **2004**, *16*, 1838−1841.
(23) Scaffardi, L. B.; Tocho, J. O. *Nanotechnology* **2006**, *17*, 1309−1315.
(24) Lu, Y.; Yin, Y. D.; Li, Z. Y.; Xia, Y. N. *Nano Lett.* **2002**, *2*, 785−788.
(25) Ding, B.; Lee, B. J.; Yang, M. J.; Jung, H. S.; Lee, J. K. *Adv. Energy Mater.* **2011**, *1*, 415−421.
(26) Su, K. H.; Wei, Q. H.; Zhang, X.; Mock, J. J.; Smith, D. R.; Schultz, S. *Nano Lett.* **2003**, *3*, 1087−1090.
(27) Jain, P. K.; Lee, K. S.; EI-Sayed, I. H.; EI-Sayed, M. A. *J. Phys. Chem. B* **2006**, *110*, 7238−7248.
(28) Wokaun, A.; Lutz, H. P.; King, A. P.; Wild, U. P.; Ernst, R. R. *J. Chem. Phys.* **1983**, *79*, 509−514.